Density Functional Theory Study of Anticancer/Nanocone in Biological Interaction

Najibzadeh Vameghabadi, Yasaman; Sheikhhosseini, Enayatollah*+; Akhgar, Mohammad Reza; Ahmadi, Sayed Ali

Department of Chemistry, Kerman Branch, Islamic Azad University, Kerman, I.R. IRAN

ABSTRACT: *In this research, the potential and capability of carbon NanoCones (NC) as an Olaparib carrier in the gas phase has been investigated using quantum mechanical calculations. The adsorption mechanism was studied systematically using a DFT approach and the basis sets of B3LYP/6-311+G, 6-311++G(d), and 6-311++G(d,p). According to the calculations data, the drug can be transported and carried by carbon nanocone with strong and powerful chemical adsorption with a suitable and high energy value. Coating Olaparib onto carbon nanocones will lead to more disability and reduced toxicity of the drugs in the human body, resulting in greater bioavailability. Chemical parameters like softness, hardness, chemical potential, and electrophilicity of olaparib have been calculated showing that olaparib has potent chemical activity in biochemical medium.*

KEYWORDS: *Nanocone; Computational Chemistry; DFT; Anticancer; Drug.*

INTRODUCTION

It has been shown that physiological status can affect the pharmacological and physicochemical properties of biologically active drugs [1, 2]. Drug delivery systems (DDS) provide conditions that improve drug efficiency and protect them from inactive until they reach their target sites [3]. In addition, such systems can minimize the side effects of the drug. The most common DDSs are liposomes, polymers, dendrimers, and nanoparticles [4].

Nanoparticles can carry therapeutic agents while also being tailored to specific targets. One of the most well-known nanostructures is carbon nanotubes (CNTs), which are hollow cylinders described as seamless rolled graphene sheets. Classified into single-walled (SWCNT), double-walled (DWCNT), and multi-walled (MWCNT) types, they have attracted a lot of attention after being discovered by Ijima [5]. The unique features of CNTs utilized in medical fields, while having nanometer sizes, are their high surface area/volume ratios and ability to carry chemicals [6-8]. With intriguing characteristics and unique structure [9], CNTs may be loaded with therapeutic chemicals binding covalently and making supramolecular assemblies. Interestingly, they can interact with the cell membrane and penetrate the cell during an endocytosis-dependent process, causing the cell to absorb more of the drug's composition. They also decrease the cell's resistance to drug entering limits, providing new potentials for their application in nanomedicine and nanobiotechnology [10-15]. However, pristine CNTs cannot deliver drugs because they are hydrophobic and cannot be dispersed in most solvents and biological environments. To increase the solubility and biocompatibility of CNTs, researchers have improved them in a variety of processes [16-18], including

***** *To whom correspondence should be addressed.*
+ E-mail: sheikhhosseiny@gmail.com & sheikhhosseini@iauk.ac.ir
1021-9986/2022/8/2628-2634 9/$/5.09

covalent and non-covalent functionalizing as well as encapsulation and defect modification. Exposing CNTs to oxidative conditions leads to carboxylic functional groups created along their sidewalls. Recent investigations reveal that with excellent biocompatibility, carboxylated carbon nanotubes (c-CNTs) can facilitate targeting therapy [19]. Inorganic nanostructures such as nanocones, nanosheets, nano chains, nanotubes, as well as nanoclusters are currently considered by researchers due to their exceptional stability in terms of thermal and chemical properties, along with their extraordinary mechanical as well as electronic features [20-45]. In the present work, nanocone interaction parameters are calculated theoretically. Nanocone is used as a drug carrier. The interaction of Olaparib with nanocones is examined using the DFT technique B3LYP/6-311+G, 6-311++G(d), and 6-311++G(d,p) by Gaussian 03 software. The novelty of this work is using nanocone as a kind of nanocarrier.

COMPUTATIONAL METHODS

Quantum mechanics calculation

In this study, Olaparib (Ola) adsorption behavior on nanocone was investigated. Theoretical quantum chemical computations were executed by exploiting the Gaussian 09 software package [46]. Using the DFT approach and the basis sets of B3LYP/6-311+G, 6-311++G(d), and 6-311++G(d,p), the equilibrium geometries were fully optimized, and their electronic densities and total energies were calculated. The adsorption energies of Olaparib on the most active sites of nanocone were calculated using Eq. (1):

$$E_{ads} = E_{T(EOla-NC)} - (E_{TNC} + E_{TOla}) \quad (1)$$

Where $E_{T(TNC)}$ and $E_{T(Ola)}$ represent the total energy of nanocone and Olaparib, respectively, and $E_{T(EOla-NC)}$ demonstrates the total energy of the Olaparib-nanocone. No imaginary frequencies in the vibrational spectra of the studied structures ascertain their stability. The molecular charge distribution was assessed according to the molecular electrostatic potential (MEP) energy surface. Besides, the DFT-based reactivity descriptors were evaluated using the Frontier Molecular Orbital (FMO) theory [47–50]. Thus the chemical reactivity and stability descriptors as the electronic chemical potential (μ), the chemical hardness (η), the chemical softness (S), and the electrophilicity were calculated based on Koopmans theorem (Eqs. 2–5):

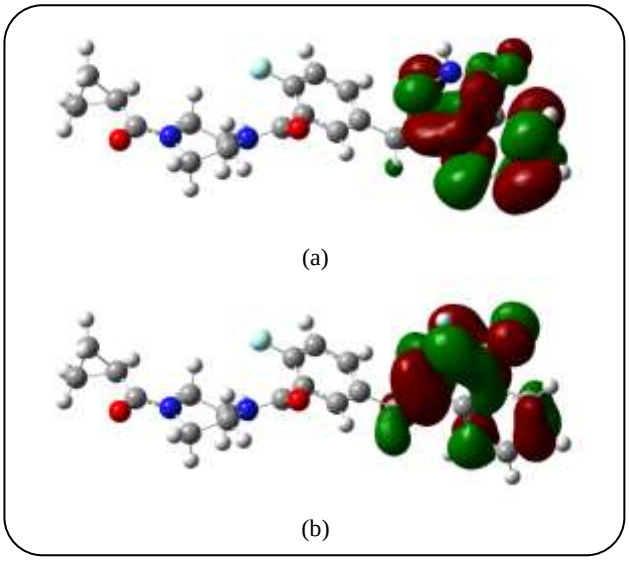

Fig 1: a) LUMO and b) HOMO plots of Olaparib

$$\mu = -\chi \quad (2)$$

$$\eta = \left(\frac{I - A}{2}\right) \quad (3)$$

$$S = 1/\eta \quad (4)$$

$$\omega = \chi^2/2\eta \quad (5)$$

Where μ, η, S, and ω are the chemical potential, the chemical hardness, the global softness, and the electrophilicity index, respectively.

RESULTS AND DISCUSSION

To assess the stability of the Ola-NC complex and to find its minimum energy point, first, the Olaparib (Ola) and nanocone (NC) structures were individually optimized, and then the proposed structure of the Ola-NC complex was optimized based on the DFT computational method. The optimized structure of Ola and its HOMO/LUMO levels are shown in Figs. 1a and 1b, respectively, and the predicted energies are provided in Table 1.

Tables 2 and 3 have compared some selected parameters between Ola's pre-adsorbed and post-adsorbed structures. The frontier molecular orbitals (FMOs), i.e., the highest occupied molecular orbital (HOMO), and the lowest unoccupied molecular orbital (LUMO) have important functions in molecular reactivity and stability.

The more HOMO-LUMO energy gap, the more molecule's kinetic stability, and its less chemical reactivity. The schematics of these orbitals were generated *via* Gauss View 5.0 software and are shown in Fig. 1.

Table 1: Energy data of Ola, NC, and Ola/NC by B3LYP/6-311+G, 6-311++G(d), and 6-311++G(d,p).

	E (6-311+G)	E(6-311++G(d))	E(6-311++G(d,p))	E(HOMO)	E(LUMO)
Ola	-3867.60	-3867.65	-3867.68	-0.24799	-0.07081
NC	-18230.66	-18230.75	-18230.85	-0.19838	-0.04190
Ola/NC	-9583.45	-9584.38	-9584.31	-0.20506	-0.02111

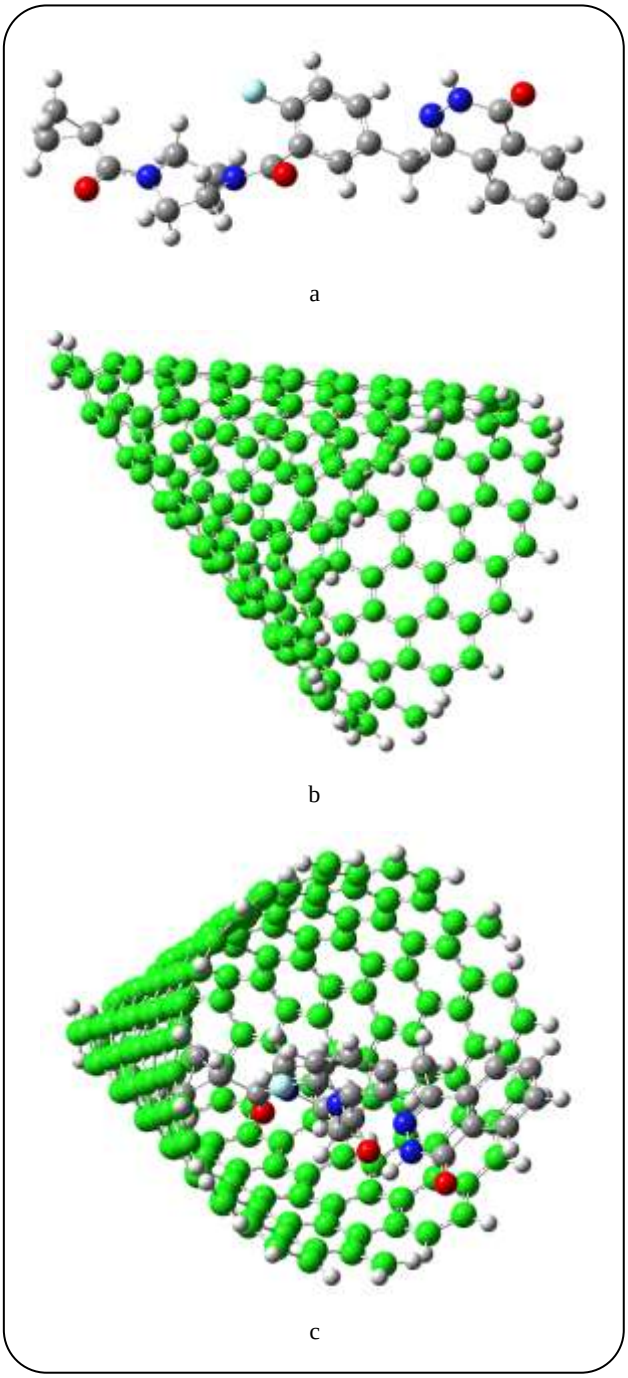

Fig. 2: Optimized structure of a) Ola, b) NC, and c) complex of Ola/NC.

Table 2: Bond length (Å) of Ola after and before the adsorption.

	Bond length (Å)	
	Before	After
N15-N16	1.37	1.34
C7-O14	1.25	1.21
N15-C8	1.31	1.29
N15-H13	1.008	1.005
N38-C29	1.36	1.34

Table 3: Angle (˚) of Ola after and before the adsorption.

	Angle (˚)	
	Before	After
O14-C7-N15	120.79	120.75
N16-N15-H13	38.55	38.53
C3-C7-O14	29.65	29.63

The nucleophilic and electrophilic active sites of Ola were investigated based on the molecular electrostatic potential (MEP) surfaces computed by the DFT approach and B3LYP/6-311++G(d,p) basis set. According to Fig. 3, different colors have been used to point the sites that differed in the electrostatic potential value: the points with the most negative and the most positive electrostatic potentials are specified with red and green colors, respectively, and the gray color indicates the points with the zero electrostatic potential.

Figs. 3 a and b show the optimized geometry and the molecular graph of NC, respectively. The greater negative electron density at the double bond critical points demonstrates the covalent bond. The approximation of Ola and NC to each other leads to different electrostatic potentials at their surfaces. In Fig. 1, the NC regions with attraction or repulsion potentials have been visualized in red and blue colors, respectively. The Gauss View 5.0 software was exploited for constructing the molecular electrostatic potential map and the electron density isosurface.

Table 4: Some of the important chemical parameters (eV).

Molecular parameters	Ola	NC	Ola/NC
E HOMO	-0.24799	-0.19838	-0.20506
E LUMO	-0.07081	-0.04190	-0.02111
ΔE HOMO-LUMO	-0.17718	-0.15648	-0.18395
IP(ioniziation energy)	0.24799	0.19838	0.20506
Electron affinity(EA)	0.07081	0.04190	0.02111
Electronegativity(χ)	0.1594	0.12014	0.113085
Chemical potential(μ)	-0.1594	-0.12014	-0.113085
Chemical softness(s)	11.2879557	12.78118609	10.87251971
Chemical hardness(η)	0.08859	0.07824	0.091975
Global electrophilicitiyindex(ω)	0.1434042	0.09223	0.06952

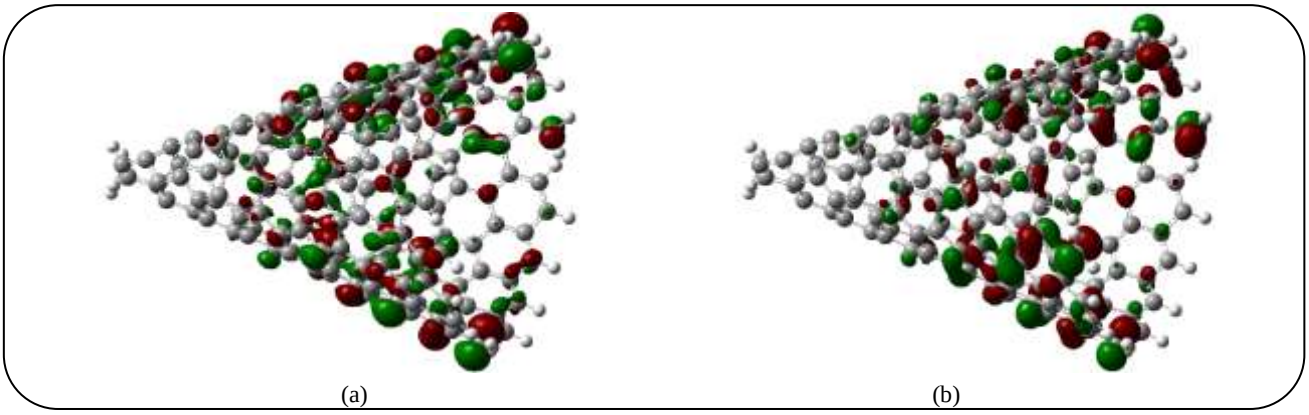

Fig 3: a) HOMO and b) LUMO Plot of nanocone.

Consequently, the same theoretical approach has been used for the Ola-NC complex. The Ola adsorption to the NC is conducted via the carbon groups. Resulted of the negative adsorption energy, the complete, relaxation of the Ola-NC complex leads to stable adsorption. It should be noted that during the adsorption process, the bond position is steady, and only its length is increased. The binding energy for the energetically favorable complex and the equilibrium distance in the interaction zone C-O…N-N and N-H…O-C respectively in the obtained results indicate the strong chemisorption that occurred and the elongated bonds in the interaction zone. The optimized geometry of Ola loaded on NC is shown in Fig. 2 from front and side views. Having no spatial and geometrical limitations, the adsorption didn't alter the geometry of the drug, and it doesn't deform significantly. LUMO and HOMO orbitals are localized through the NC framework with no distribution of the Ola, and their energy levels are slightly different than those of the individual NC. Table 4 shows the DFT-based quantum chemical parameters calculated using Eqs. (2–5). The reduced ionization potential and energy gap of Ola-NC indicate its more reactivity. Furthermore, the computed data shows the raised electrophilicity of Ola-NC, proposing a decrease in charge transfer from Ola to NC. As two essential parameters indicating stability and reactivity, the global chemical hardness and softness have been calculated. The reduced Ola-NC hardness demonstrates its higher reactivity.

CONCLUSIONS

High drug loading, thermal ablation, and structural stability have received our effort to investigate the

theoretical study of its potential as a carrier for olaparib. The adsorptions of Ola on the NC site via different active sites have been studied. We found that Ola could strongly be adsorbed in NC. Because of the high surface area and H and C-bonding, the adsorption efficiency of c- was stable, and we hope the preparation of such efficient drug carriers overcomes the limitations of Ola and facilitates targeting.

Received : Mar. 1, 2022 ; Accepted : Jul. 4, 2022

REFERENCES

[1] Yoosefian M., Jahani M., A Molecular Study on Drug Delivery System Based on Carbon Nanotube for the Novel Norepinephrine Prodrug, Droxidopa, *J. Mol. Liq*, **284**: 258-264 (2019).

[2] Olanow C.W., Stern M.B., Sethi K., The Scientific and Clinical Basis for the Treatment of Parkinson Disease, *Neurology*, **72**: S1-S136 (2009).

[3] Vashist S.K., Zheng D., Pastorin G., Al-Rubeaan K., Luong J.H., Sheu F.S., Delivery of Drugs and Biomolecules Using Carbon Nanotubes, *Carbon*, **49**: 4077-4097 (2011).

[4] Portney N.G., Ozkan M., Nano-oncology: Drug Delivery, Imaging, and Sensing, *Anal. Bioanal. Chem*, **384**: 620-630 (2006).

[5] Ajayan P.M., Lambert J.M., Bernier P., Barbedette L., Colliex C., Planeix J.M., Growth Morphologies During Cobalt-catalyzed Single-shell Carbon Nanotube Synthesis, *Chem. Phys. Lett.*, **215**: 509-517 (1993).

[6] Yoosefian M., Etminan N., The Role of Solvent Polarity in the Electronic Properties, Stability and Reactivity Trend of a Tryptophane/Pd Doped SWCNT Novel Nanobiosensor from Polar Protic to Non-polar Solvents, *RSC Adv*, **6**: 64818-64825 (2016).

[7] Rahmanifar E., Yoosefian M., Karimi-Maleh H., Electronic Properties and Reactivity Trend for Defect Functionalization of Single-walled Carbon Nanotube with B, Al, Ga Atoms, *Synth. Met*, **221**: 242-246 (2016).

[8] Yoosefian M., Etminan N., Leucine/Pd-loaded (5, 5) Single-walled Carbon Nanotube Matrix as a Novel Nanobiosensors for in Silico Detection of Protein, *J. Amino Acids*, **50**: 653-661 (2018).

[9] Tiwari A., Mishra Y.K., Kobayashi H., Turner A.P., "Intelligent Nanomaterials", John Wiley & Sons, Inc. (2016).

[10] Pantarotto D., Singh R., McCarthy D., Erhardt M., Briand J.P., Prato M., Kostarelos K., Bianco A., Functionalized Carbon Nanotubes for Plasmid DNA Gene Delivery, *Angew. Chem. Int. Ed*, **43**: 5242-5246 (2004).

[11] Etminan N., Yoosefian M., Raissi H., Hakimi M., Solvent Effects on the Stability and the Electronic Properties of Histidine/Pd-doped Single-walled Carbon Nanotube Biosensor, *J. Mol. Liq.*, **214**: 313-318 (2016).

[12] Yoosefian M., Etminan N., Pd-doped Single-Walled Carbon Nanotube as a Nanobiosensor for Histidine Amino Acid, a DFT Study, *RSC Adv.*, **5**: 31172-31178 (2015).

[13] Sanghavi B.J., Mobin S.M., Mathur P., Lahiri G.K., Srivastava A.K., Biomimetic Sensor for Certain Catecholamines Employing Copper (II) Complex and Silver Nanoparticle Modified Glassy Carbon Paste Electrode, *Biosens. Bioelectron*, **39**: 124-132 (2013).

[14] Balasubramanian K., Burghard M., Biosensors Based on Carbon Nanotubes, *Anal. Bioanal. Chem*, **385**: 452-468 (2006).

[15] Jianrong C., Yuqing M., Nongyue H., Xiaohua W., Sijiao L., Nanotechnology and Biosensors, *Biotechnol. Adv*, **22(7)**: 505-518 (2004).

[16] Chen R.J., Zhang Y., Wang D., Dai H.J., Organic Functionalization of Carbon Nanotubes, *J. Am. Chem. Soc*, **123(16)**: 3838-3839 (2001).

[17] Yoosefian M., Mola A., Fooladi E., Ahmadzadeh S., The Effect of Solvents on Formaldehyde Adsorption Performance on Pristine and Pd Doped on Single-walled Carbon Nanotube Using Density Functional Theory, *J. Mol. Liq*, **225**: 34-41 (2017).

[18] Yoosefian M., Applied Surface Science a High Efficient Nanostructured Filter Based on Functionalized Carbon Nanotube to Reduce the Tobacco-specific Nitrosamines, *Appl. Surf. Sci*, **434**: 134-141 (2018).

[19] Chen Z., Pierre D., He H., Tan S., Pham-Huy C., Hong H., Huang J., Adsorption Behavior of Epirubicin Hydrochloride on Carboxylated Carbon Nanotubes, *Int. J. Pharm*, **405(1-2)**: 153-161 (2011).

[20] Peyghan A.A., Soleymanabadi H., Computational Study on Ammonia Adsorption on the X 12 Y 12 Nano-Clusters (x = B, Al and Y = N, P), *Curr. Sci*, **108(10)**:1910-1914 (2015).

[21] Beheshtian J., Peyghan A.A., Bagheri Z., Functionalization of BN Nanosheet with N_2H_4 May be Feasible in the Presence of Stone–Wales Defect, *Struct. Chem*, **24**:1565–1570 (2013).

[22] Samadizadeh M., Rastegar S.F., Peyghan A.A., F^-, Cl^-, Li^+ and Na^+ Adsorption on AlN Nanotube Surface: A DFT Study, *Phys. E Low-dimens. Syst. Nanostruct.*, **69**:75–80 (2015).

[23] Rostami Z., Soleymanabadi H., Investigation of Phosgene Adsorption Behavior on Aluminum Nitride Nanocones: Density Functional Study, *J. Mol. Liq*, **248**:473–478 (2017).

[24] Beheshtian J., Peyghan A.A., Bagheri Z., Kamfiroozi M., Interaction of Small Molecules (NO, H_2, N_2, and CH4) with BN Nanocluster Surface, *Struct. Chem.*, **23**:1567–1572 (2012).

[25] Bagheri Z., Peyghan A. A., DFT Study of NO_2 Adsorption on the AlN Nanocones, *Comput. Theor. Chem*, **1008**:20–26 (2013).

[26] Moradi A.V., Peyghan A.A., Hashemian S., Baei M.T., Theoretical Study of Thiazole Adsorption on the (6,0) Zigzag Single-Walled Boron Nitride Nanotube, *Bull. Korean Chem. Soc*, **33**:3285–3292 (2012).

[27] Beheshtian J., Soleymanabadi H., Peyghan A.A., Bagheri Z., A DFT Study on the Functionalization of a BN Nanosheet with PC Single BondX, (PC = Phenyl Carbamate, X = OCH_3, CH_3, NH_2, NO_2 and CN), *Appl. Surf. Sci*, **268**:436–441 (2012).

[28] Baei M.T., Taghartapeh M.R., Lemeski E.T., Soltani A., A Computational Study of Adenine, Uracil, and Cytosine Adsorption upon AlN and BN Nano-cages, *Phys. B.*, **444**:6–13 (2014).

[29] Beheshtian J., Peyghan A.A., Tabar M.B., Bagheri Z., DFT Study on the Functionalization of a BN Nanotube with Sulfamide, *Appl. Surf. Sci*, **266**: 182–187 (2013).

[30] Vessally E., Behmagham F., Massoumi B., Hosseinian A., Edjlali L., Carbon Nanocone as an Electronic Sensor for HCl Gas: Quantum Chemical Analysis, *Vacuum.*, **134**:40–47 (2016).

[31] Gholami A., Hashemi S.A., Yousefi K., Mousavi S.M., Chiang W.H., Ramakrishna S., Mazraedoost S., Alizadeh A., Omidifar N., Behbudi G., Babapoor A., 3D Nanostructures for Tissue Engineering, Cancer Therapy, and Gene Delivery, *J. Nanomater*, **2020**: 1852946 (2020).

[32] Masoumzade R., Behbudi G., Mazraedoost S., A Medical Encyclopedia with New Approach Graphene Quantum Dots for Anti-breast Cancer Applications: Mini Review, *J. Adv. in Appl. NanoBio Tech*, **1(4)**:84-90 (2020).

[33] Goudarzian N., Amini P., Mousavi S.M., Hashemi S.A., Modification of Physical, Mechanical and Electrical Properties of Reinforced Epoxy Phenol Novolac with Nano Cobalt Acrylate and Carbon Nanotubes, *Prog. Rubber Plast. Recycl. Technol*, **34(2)**: 105-114 (2018).

[34] Amani A.M., Hashemi S.A., Mousavi S.M., Abrishamifar S.M., Vojood A., "Carbon Nanotubes-recent Progress", ed. by Rahman M.M., Asiri A.M., (2017).

[35] Hashemi S.A., Mousavi S.M., Arjmand M., Yan N., Sundararaj U., Electrified Single-walled Carbon Nanotube/epoxy Nanocomposite via Vacuum Shock Technique: Effect of Alignment on Electrical Conductivity and Electromagnetic Interference Shielding, *Polym. Compos*, **39(S2)**:E1139-E1148 (2018).

[36] Hashemi S.A., Mousavi S.M., Effect of bubble based degradation on the physical properties of Single Wall Carbon Nanotube/Epoxy Resin Composite and New Approach in Bubbles Reduction, *Compos. Part A Appl. Sci. Manuf*, **90**:457-469 (2016).

[37] Karimi-Maleh H., Karimi F., Fu L., Sanati A.L., Alizadeh M., Karaman C., Orooji Y. Cyanazine Herbicide Monitoring as a Hazardous Substance by a DNA Nanostructure Biosensor, *J. Hazard. Mater*, **423**: 127058 (2022).

[38] Karimi-Maleh H., Tahernejad-Javazmi F., Ensafi A.A., Moradi R., Mallakpour S., Beitollahi H. A High Sensitive Biosensor Based on FePt/CNTs Nanocomposite/N-(4-hydroxyphenyl)-3,5-dinitrobenzamide Modified Carbon Paste Electrode for Simultaneous Determination of Glutathione and Piroxicam, *Biosens. Bioelectron*, **62**: 1-7 (2014).

[39] Karimi-Maleh H., LütfiYola M., Atar N., Orooji Y., Karimi F., Kumar P.S., Rouhi J., Baghayerii M., A Novel Detection Method for Organophosphorus Insecticide Fenamiphos: Molecularly Imprinted Ilectrochemical Sensor Based on Core-shell Co_3O_4@MOF-74 Nanocomposite, *J. Colloid Interface Sci*, **592**: 174-185 (2021).

[40] Nazar Ali Z., Ahmadi S.A., Ghazanfari D., Sheikhhosseini E., Razavi R. Investigation of Flutamide@Ethyleneimine as Drug Carrier by Nanocone and Nanotube Theoretically, *Iran. J. Chem. Chem. Eng. (IJCCE)*, **41(10)**: 3275-3281 (2022).

[41] Chafai N., Benbouguerra K., Chafaa S., Quantum Chemical Study of Hydroxychloroquine and Chloroquine Drugs Used as a Treatment of COVID-19, *Iran. J. Chem. Chem. Eng. (IJCCE)*, **41(1)**: 27-36 (2022).

[42] Aramesh-Boroujeni Z., Jahani S. Computational and Experimental Study on the Interaction of Terbium (III) and Ytterbium (III) Complexes Containing 1,10-phenanthroline with Bovine Serum Albumin, *Iran. J. Chem. Chem. Eng. (IJCCE)*, **41(1)**: 58-70 (2022).

[43] Vessally E., Musavi M., Poor Heravi M., A Density Functional Theory Study of Adsorption Ethionamide on the Surface of the Pristine, Si and Ga and Al-Doped Graphene, *Iran. J. Chem. Chem. Eng. (IJCCE)*, **40(6)**: 1720-1736 (2021).

[44] Vessally E., Farajzadeh P., Najafi E. Possible Sensing Ability of Boron Nitride Nanosheet and Its Al– and Si–Doped Derivatives for Methimazole Drug by Computational Study, *Iran. J. Chem. Chem. Eng. (IJCCE)*, **40(4)**: 1001-1011 (2021).

[45] Tavakoli, S., Ahmadi S.A., Ghazanfari D., Sheikhhosseini E., Theoretical Investigation of Functionalized Fullerene Nano Carrier Drug Delivery of Fluoxetine, *J. Indian Chem. Soc*, **99(7)**: 100561 (2022).

[46] Frisch M.J., Trucks G.W., Schlegel H.B., Scuseria G.E., Robb M.A., Cheeseman J.R., Nakatsuji H., Gaussian D.V., Revision H. 10. Gaussian. Inc. Wallingford, CT (2010).

[47] Brovarets O.H.O., Zhurakivsky R.O., Hovorun D.M., The Physico-chemical Mechanism of the Tautomerization Via the DPT of the Long Hyp* Center Dot Hyp Watson-Crick Base Pair Containing rare Tautomer: A QM and QTAIM Detailed Look, *Chem. Phys. Lett*, **578**: 126-132 (2013).

[48] Ol'ha O.B., Voiteshenko I.S., Perez-Sanchez H., Hovorun D.M., A QM/QTAIM Research Under the Magnifying Glass of the DPT Tautomerisation of the Wobble Mispairs Involving 2-Aminopurine, *New J. Chem*, **41**: 7232-7243 (2017).

[49] Ol'ha O.B., Hovorun D.M., By How Many Tautomerisation Routes the Watson–Crick-like A· C* DNA Base Mispair is Linked with the Wobble Mismatches? A QM/QTAIM Vision from a Biological Point of View, *J. Struct. Chem*, **27**: 119-131 (2016).

[50] Hovorun D.M., Can Tautomerisation of the A·T Watson–Crick Base Pair via Double Proton Transfer Provoke Point Mutations During DNA Replication? A Comprehensive QM and QTAIM Analysis, *J. Biomol. Struct. Dyn*, **32(1)**: 127-154 (2014).